Interactions between Geometry and Mechanical Properties on the Optic Nerve Head

Ian A. Sigal

PURPOSE. To determine the relative strength, independently and in interaction, of the influence of factors representing the geometry and mechanical properties on the IOP-induced stresses and strains within the optic nerve head (ONH).

METHODS. A computational model of the eye was developed such that 21 factors could be varied independently or simultaneously. A fractional factorial screening analysis was used to identify the factors and interactions with the largest influences on the lamina cribrosa (LC) and prelaminar neural tissue (PLNT).

RESULTS. Nine factors and their interactions accounted for the majority of the variance in the responses (between 95% and 99.8%). These factors were: the properties of the sclera (modulus, eye radius, and shell thickness), LC (modulus and radius), PLNT (modulus and compressibility), and optic nerve (modulus), and IOP. The interactions were stronger on the PLNT than on the LC (up to 16.4% and 9.0% of the response variances, respectively). No factor was the most influential on all the responses or sufficient to ensure high or low levels of strain or stress. Although the modulus of the sclera was among the most influential factors, its effects could be outweighed by other factors.

CONCLUSIONS. There were strong interactions between and within the geometry and mechanical properties of the tissues of the ONH. This suggests that to ascertain individual susceptibility to IOP it may be necessary to determine several properties of the eye, as well as their interactions. The influential factors and their covariances should be better characterized. (*Invest Ophthalmol Vis Sci.* 2009;50:2785–2795) DOI:10.1167/iovs.08-3095

Glaucoma is one of the leading causes of blindness worldwide.[1] Although elevated intraocular pressure (IOP) is the primary risk factor for the development of the disease, the mechanisms by which elevated IOP eventually leads to damage and loss of neural function are still unclear and remain controversial.[2,3] The controversy is due in part to the wide range of individual sensitivities to elevated IOP. Several recent publications have explored the hypothesis that IOP-induced forces and deformations (stresses and strains) of the tissues of the optic nerve head (ONH) and, in particular, the lamina cribrosa (LC) contribute to the pathogenesis of the disease.[2,4–7] Within this framework, the range of sensitivities to IOP are proposed to be due, at least in part, to differences between individuals in geometry and mechanical properties of the tissues of the ONH. Therefore, to understand individual susceptibility to IOP it is necessary to determine how ONH biomechanics is influenced by the tissue geometry and mechanical properties.

Unfortunately, direct measurement of the ONH biomechanical environment is challenging at present, and alternate approaches are therefore needed. One such approach is modeling. Several analytical[5,8,9] and computational[6,10,11] models have been developed for this purpose. A previous study examined the influence on ONH biomechanics of 21 factors spanning the geometry, mechanical properties, and loading, and found that ONH biomechanics were influenced most strongly by scleral stiffness and thickness.[12] Other factors such as eye size and LC mechanical properties were also influential, but to a lesser degree. Equivalent results were obtained across several aspects of the ONH response, even when the factor ranges were varied. Nevertheless, the analysis has some important limitations because it was performed with a one-factor-at-a-time (OFAT) technique. In OFAT, starting from a baseline configuration, factors are varied one at a time, while keeping all others constant. OFAT designs are common in computational biomechanics due to the simplicity in preparation and analysis.[13] OFAT studies, however, privilege the baseline, limit the combinations of factors studied, and provide no information on the possible interactions between factors (i.e., on how the effects of factors depend on each other). This limitation is potentially important because in biological systems factors are often related, vary together, and have effects that depend on each other. Factor interactions have been shown to be important in various areas of biomechanics,[14–17] and the eye is likely not an exception. To the best of the author's knowledge there are no studies of the role of factor interactions in ONH biomechanics.

The goal of this study was to determine the relative strength, independently and in interaction, of factors representing geometry and mechanical properties on the IOP-induced stresses and strains within the ONH. I hypothesized that, in posterior pole biomechanics, factor interactions are likely substantial, and therefore that it is critical to identify the most influential interactions so that they can be considered in future studies.

METHODS

The overall strategy was the following (the steps are described in more detail later): Develop a parameterized finite element (FE) model of a generic ONH such that a model with the desired combination of factor levels (a configuration) could be readily produced. A set of configurations used to sample the factors space was determined with a fractional factorial design of experiments (DOE) methodology. Each configuration model was then used to simulate an increase in IOP, and the response was characterized by the magnitudes of the strains and stresses within the LC and the prelaminar neural tissue (PLNT). Standard statistical techniques associated with the DOE method were then used to determine the relative strength of the contribution of each factor and of their interactions to the variances in the responses. Finally, the most influential factors were identified and the percentage of response variance accounted for by them and their interactions was computed.

Note the following terminology: I refer to the variables as factors, with levels, as is often done in statistics. Simulation analysts instead speak of inputs, input factors, or parameters with values. A set of factor levels determines a configuration, sometimes called a design point, a run, or a scenario. Models are built according to a configuration and used to simulate an increase in IOP. From a simulation are computed the responses, also referred to as outputs or outcome measures. I refer to the strength of the effects of factors on responses as factor main effects, direct effects, or the effects of factors independently, and of factors in conjunction, as factor interactions, or just interactions. Interactions are sometimes classified by order (e.g., zeroth, first, second) or by the number of factors (or "ways") involved (e.g., two-factor/two-way, three-factor/three-way interactions). In this work, for simplicity, interactions refers to two-factor interactions. Higher order interactions were found to have much weaker effects and are therefore not presented or discussed. Note also that the DOE technique should not be confused with the colloquial use of "design of experiments" in the literal sense.

The Model

The analysis was performed with a previously described parametric model of the ONH.[12,18] The scripts were adapted so that factors could be varied independently and simultaneously. Briefly, a 3-D axisymmetric model with geometry chosen to represent an idealized generic human eye was developed. The ONH was modeled in some detail, whereas the rest of the eye was modeled as a spherical shell of constant thickness. Five tissue regions were defined: corneoscleral shell, LC, prelaminar neural tissue (PLNT, including the retina and choroid), postlaminar neural tissue (ON, including the optic nerve), and pia mater. Although the models were axisymmetric, they represented a 3-D geometry, which should not be confused with a 2-D model.

Model factors, and the ranges over which they were allowed to vary, were the same as reported in prior studies.[12,19,20] The factors are illustrated in Figure 1 and their ranges listed in Table 1. All tissues were assumed linearly elastic, isotropic, and homogeneous.[12,18] All tissues, other than the PLNT, were assumed incompressible. Accordingly, tissue mechanical properties were defined by the Young's modulus of each of the five tissues and the compressibility (Poisson's ratio) of the PLNT. The choice of mechanical properties and their consequences are addressed in the Discussion section. In this work, stiff and compliant are used to describe high and low Young's moduli, respectively. In

this sense, stiffness is equivalent to the tissue's mechanical property and is independent of the geometry. IOP was represented as a homogeneous force on the interior surfaces. IOP was included as a factor to allow evaluation of the magnitude of its effects relative to other factors. The apex of the region representing the cornea was constrained in all directions to prevent displacement or rotation.

Numerical Details

Commercial FE software (Ansys ver. 8; Ansys Inc., Canonsburg, PA) was used to develop and analyze the models. The process was scripted in Ansys parametric design language. A configuration could be produced, solved, and analyzed without user intervention, typically requiring less than a minute per configuration on a desktop workstation with 3GB of RAM.

All tissue regions were meshed with eight-node elements (PLANE 82 in Ansys). Optimal element size was determined in a preliminary mesh refinement study.[19] Once sufficient element resolution was determined for a particular geometry, the resolution was quadrupled (element side length divided by 2 in each direction) to allow for the higher resolution requirements of other configurations. After the study, cases with particularly high strain or stress levels were refined and solved again to verify that the default resolution was sufficient. In every case, it was.

Responses

As responses of the FE simulations, I chose the IOP-induced maximum and minimum principal strains and the von Mises stress. The maximum and minimum principal strains represent the amount of stretching and compression that the tissue undergoes, respectively, whereas the von Mises stress represents the forces within the tissue per unit area, discounting the effects of hydrostatic pressure. For briefness these are referred to as tensile and compressive strains and stress. For each tissue, the distribution of each of the strains and stress was computed and these distributions characterized by the 50th and 95th percentiles, the median and peak. The 95th percentile was used as the definition of the peak value so as to reduce the influence of possible numerical artifacts or of regions too small to have a physiologic significance. As in previous studies,[12,18] the analysis of the PLNT was limited to the region within 5° of the axis of symmetry to focus on the ONH.
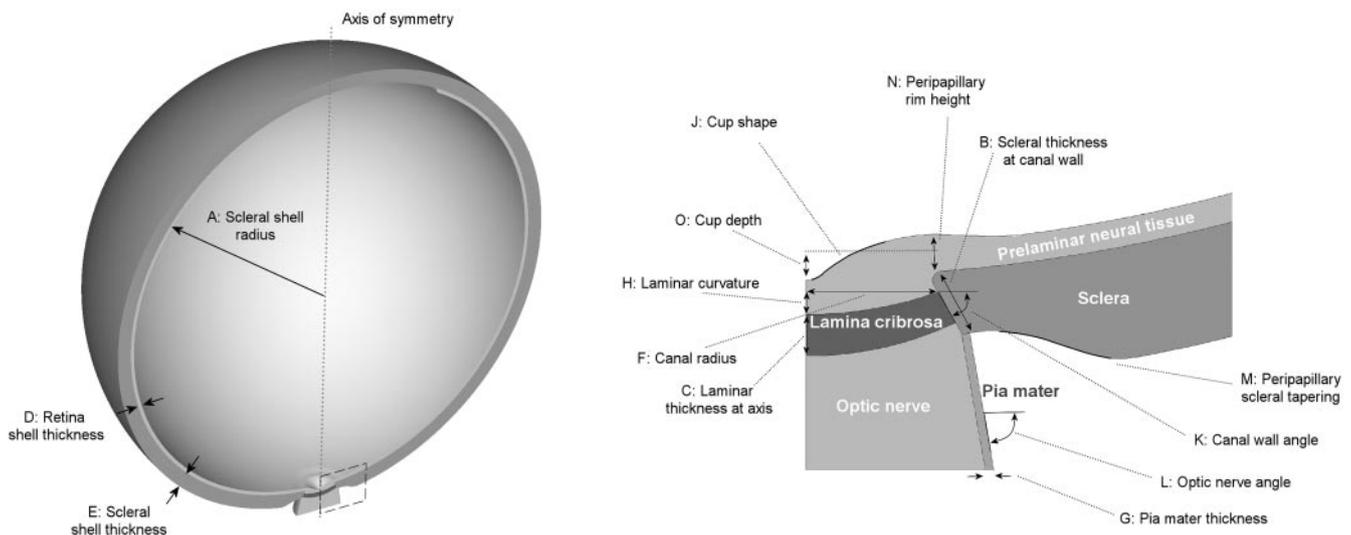
FIGURE 1. Generic axisymmetric finite element model and the geometric factors analyzed in this study. *Left*: half of the model shown in perspective with the ONH at the bottom outlined by the *dashed line*. *Right*: detail of the ONH. Five tissue regions were modeled: sclera, prelaminar neural tissue (PLNT, including the retina), lamina cribrosa (LC), postlaminar neural tissue (ON, the optic nerve), and pia mater. In addition to the geometric factors shown, IOP and six factors representing the mechanical properties of the five tissue regions were also varied. See Table 1 for factor ranges. The geometry shown is the same as was used as baseline in a previous OFAT study.[12]

TABLE 1. Factors and Their Codes and Ranges

Factor	Code	Units	Low −1	High +1
Factors defining the geometry of the eye and ONH				
Eye size (scleral shell internal radius)	A	mm	9.6	14.4
Scleral thickness (at canal wall)	B	mm	0.32	0.48
Laminar thickness at axis	C	mm	0.24	0.36
Retinal thickness (shell)	D	mm	0.16	0.24
Scleral thickness (shell)	E	mm	0.64	0.96
LC anterior surface radius	F	mm	0.76	1.14
Pia mater thickness	G	mm	0.048	0.072
LC depth at axis below rim	H	mm	0	0.2
Cup-to-disc ratio	J	—	0.1	0.5
Canal wall angle to the horizontal	K	deg	48	72
Optic nerve angle to the horizontal	L	deg	64	96
Peripapillary sclera tapering	M	—	0	1
Peripapillary rim height	N	mm	0.24	0.36
Cup depth	O	mm	0.26	0.4
Loading				
IOP	P	mm Hg	20	30
Factors defining the mechanical properties of relevant optic tissues				
PLNT compressibility (Poisson ratio)	Q	—	0.4	0.49
Pia mater stiffness (Young's modulus)	R	MPa	1	9
LC stiffness (Young's modulus)	S	MPa	0.1	0.9
Sclera stiffness (Young's modulus)	T	MPa	1	9
PLNT stiffness (Young's modulus)	U	MPa	0.01	0.09
ON stiffness (Young's modulus)	V	MPa	0.01	0.09

See Figure 1 for factor definitions.

Choosing Factor Combinations

To sample the 21-dimension factor space efficiently, a two-level fractional factorial 2^{21-12} design requiring 512 configurations was selected.[21,22] The factor configurations formed an orthogonal array, which means that all factors were distributed in a balanced manner, with an equal number of occurrences of low and high levels for each factor. For example, there were as many configurations with low (256) LC modulus as with high (256) LC modulus (Fig. 2). The order in which the configurations were preprocessed, simulated, and analyzed was randomized. Ten replicates of a central point configuration (all factors at the midpoint between low and high levels) were added to the design and randomly inserted in the run sequence to check for pure error. Pure error is a measure of the variance intrinsic to the method. In deterministic studies, such as this one, pure error should be zero because of the perfect repeatability of the simulations. Pure error could be nonzero if there had been any drift in the predictions from one simulation to the next. For all the responses, pure error was zero.

Analysis

An analysis of variance (ANOVA) was used to determine the statistical significance of the factor and interaction effects, as is standard in DOE.[15,21] For each response, the percentage of the total sum of squares corrected by the mean was used to represent the approximate contribution of each factor and interaction to the variance of the response, providing a measure of influence, as is usual in factor analysis.[21,23] All factors influenced the responses to some degree, but some of these influences were either very small, or not statistically significant. To be deemed influential, a factor had to contribute at least 5% to the total variance of a response. Interactions had to contribute at least 5% of the variance in a response due to all interactions. To be influential, the contribution of a factor or interaction also had to be statistically significant ($P < 0.01$) and greater than the residual. The residual was the portion of the corrected total sum of squares that was not accounted for by the factors considered, similar to the R^2 measure in a correlation.[21,24] The residual was also used to determine confidence
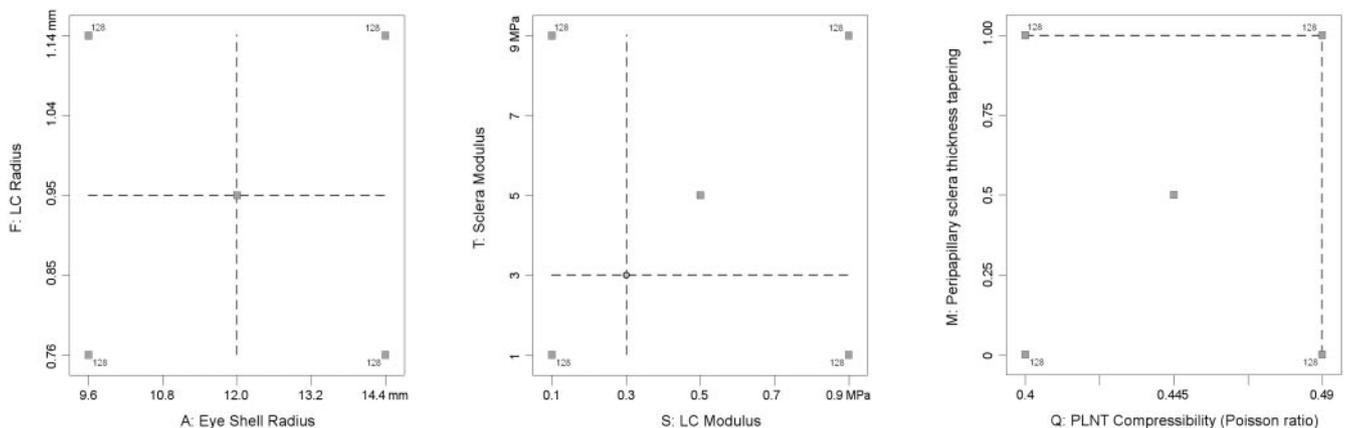

FIGURE 2. Combinations of factors, or configurations. The factors space has 21 dimensions (one for each factor studied). Shown are three 2-D projections, with a configuration shown as a small square. All configurations, except the center, were at the corners of the factor space, so that 128 configurations overlap at each corner. *Dashed lines*: cross-sections of the factor space sampled in the OFAT study reported in Ref. 12, that intersect at the baseline configuration (the geometry shown in Fig. 1). Given the factor values of the baseline configuration in the OFAT study, the cross-sections could be at the center (*left*), toward the side (*center*), or at the edge of the factors space (*right*), sometimes leaving large regions of the factor space unsampled.

intervals and the least-squares mean value for each factor level in interaction plots. Finally, factors could be influential by hierarchy: If an interaction between two factors was deemed influential, then both "parent" factors (i.e., the two interacting factors), were also considered influential,[22,25] although this criterion never turned any factor into an influential one. For the contribution threshold, 5% was chosen based on observations of the interaction plots (see the results section). A stricter criterion would have increased the cutoff percentage, classifying as noninfluential some interesting interactions. Conversely, a less strict criterion would have led to more interactions being classified as influential, increasing the complexity of the analysis.

The response variables were transformed to improve the normality of the responses and the residuals, to satisfy the requirements of ANOVA, and to allow factor effects to be added in an unbiased fashion.[22,26] A traditional Box-Cox analysis and plot method was used to determine the optimal transformation for each response. For all responses, it was found that the optimal transformation was a base 10 logarithm. This is equivalent to expressing the responses in decibels and is a common transformation for strain and stress in bioengineering DOE.[15] For plotting, the responses were converted back to the original scale. The experiment was designed and analyzed with commercial software (Design-Expert, ver. 7; Stat-Ease, Inc., Minneapolis, MN).

RESULTS

Independent Factor Effects

The relative strengths of the independent factor effects on the responses are shown in Figure 3. Considering all the responses, there were nine influential factors. Consistent with previous studies, it was found that the moduli of the sclera and LC were among the most influential factors and that factors related to the geometry of the disc cup only had a marginal influence.[12,18] In contrast with previous studies, there were several responses for which other factors were more influential than the sclera, most notably the properties of the PLNT.

Note that interactions affect the way factors act on the responses, and therefore, when interactions are present, factor effects should be interpreted carefully. This is illustrated in Figure 4, where increases in either scleral or LC modulus are shown to lead to lower strains, as could be expected from findings in previous studies.[12] However, there were some rather surprising results: Even when both the sclera and LC were compliant, the magnitude of the strains could be low. Similarly, strains could be high when only the sclera or the LC were stiff. Only when both tissues were simultaneously stiff

were the strains guaranteed low. This was due to the influence of interactions whereby the effects of the scleral and LC moduli depend on each other and on other factors. Note that the high magnitudes of strain for some factor combinations are unlikely to be physiologic. This suggests that some of the configurations considered in the experimental design may be outside of physiologic ranges. This is addressed later in the discussion.

Effects of Factors in Interaction

Figure 5 shows the strengths of factor interactions. All the responses were, to some extent, affected by interactions involving properties of the sclera. However, there were substantial differences in how responses were influenced by interactions. IOP did not interact with any other factor, as should be expected, given the assumption of linear mechanical properties. The result supports the hypothesis that the design is capturing factor interactions properly. It could seem from Figure 5 that the interactions have relatively weak influences. But recall that these are global measures (i.e., over the whole factor space). Of the interactions shown in Figure 5, some had a modest influence over the whole factor space; others had an influence concentrated in a small region.

An improved understanding of the role of factor interactions can be gained by examining the interaction plots in Figures 6 to 9, which show the effects of some representative interactions on the responses. An interaction plot shows the effects of two factors on a response, with all other factors constant. Influential factors appear as steep lines, or as a wide separation between the lines. Nonparallel lines indicate that the effect of one factor depends on the other (i.e., an interaction). Line endpoints are the mean responses for a given value of the factors, whereas the error bars depict the 95% least significant confidence interval.[22] Response ranges were chosen so as to make the interactions clearest. The interaction plots were grouped according to the response: tensile strains in Figures 6 and 7 (separated depending on whether the interactions involve the sclera or not), compressive strains in Figure 8, and stress in Figure 9.

Interaction Plots of the Tensile Strain

The interaction plots in Figure 6 illustrate two recurring trends: First, whenever there was an interaction involving scleral properties, the scleral modulus was involved; second, depending on whether the sclera was stiff or compliant, the effects of some
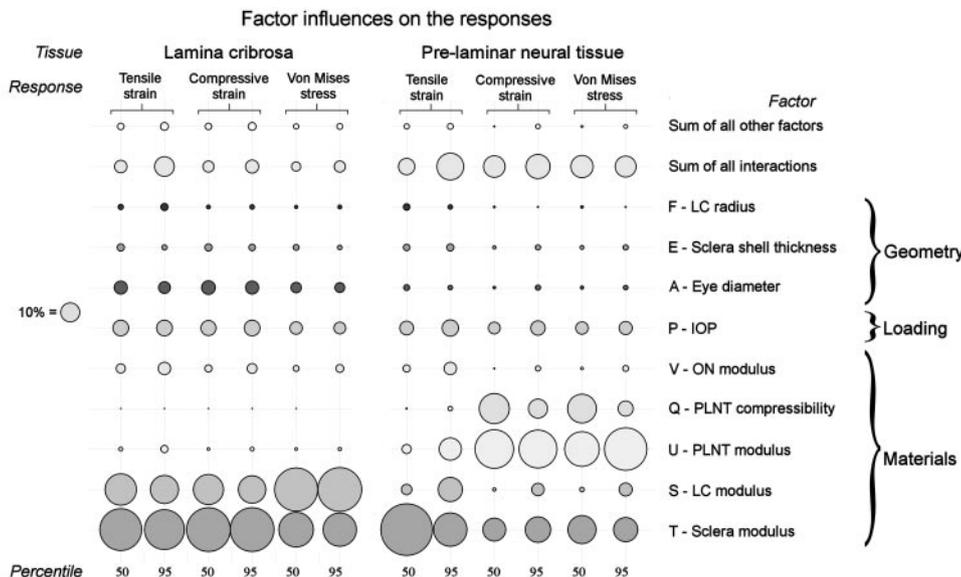
FIGURE 3. Proportion of factor influence on each response variance. Disc areas are proportional to the percentage of a response (*columns*) variance due to each of the factors (*rows*), such that larger discs represent a stronger sensitivity of the response to the factor. A factor is shown explicitly if it was deemed influential on any response. Over all the responses, there were nine such factors. The rest of the independent factors and all the factor interactions are shown aggregated in the *top two rows*. As a fraction of the total variance, interactions accounted for a relatively small amount. However, interactions affect the way factors act independently, and therefore when interactions are present, factor effects should be interpreted carefully.

FIGURE 4. Peak maximum tensile strain within the LC (*left*), and PLNT (*right*) as a function of sclera and LC moduli. There were 128 configurations with each combination of stiff/compliant and sclera/LC moduli, and one center (*circle*). Sclera and LC moduli were the most influential factors on the levels of tensile strain, such that increases in either scleral or LC stiffness led, on average, to lower strains (*P* < 0.0001). However, the strains could be high if only the sclera or LC were stiff, or the strains could be low when the sclera, the LC, or both were compliant.
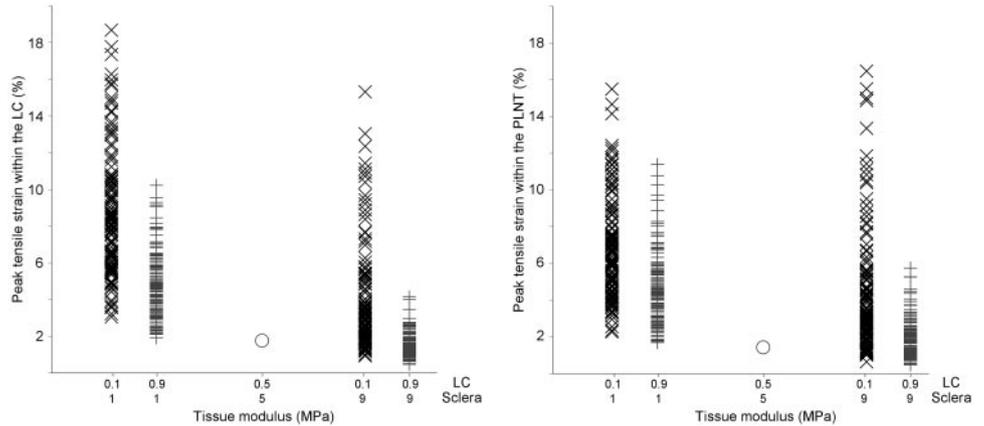
factors, such as eye size, shell thickness, and LC radius, changed, sometimes substantially, classic examples of interactions. When the sclera was stiff, neither eye size nor shell thickness had much influence on the strains within the LC or PLNT. When the sclera was compliant, either a smaller eye or a thicker scleral shell led to lower strains. The effects of increases in LC radius on the LC tensile strain were larger when the sclera was stiff than when the sclera was compliant—the result of a compliant sclera transmitting larger deformations to the LC than a stiff sclera. On the PLNT, the interaction effects were even more stark: The effects of increases of LC radius were opposite depending on the scleral modulus.

The interaction plots in Figure 7 between nonscleral factors illustrate effects of LC modulus and radius and how the ON could provide mechanical support to the LC and PLNT, if needed. As for the sclera, increased LC compliance due to a lower modulus could be compensated somewhat by the LC geometry, with a smaller LC effectively behaving stiffer. The interactions in Figure 7 were more subtle than those in Figure 6 (i.e., had a smaller effect on the magnitude of strain), but they are included as they also contribute to form a picture of ONH biomechanics.

Interaction Plots for the Compressive Strain

The compressive strains within the PLNT were also highly sensitive to interactions (Fig. 8). However, this sensitivity was

only the case for the PLNT, and the influential interactions were different from those affecting tensile strains. In another classic example of an interaction, increases in PLNT compressibility (reductions in the Poisson ratio) could lead to increases or decreases of the compressive strains within the PLNT, depending on the scleral modulus. Notably, when the PLNT was both compressible and compliant, the levels of compressive strain within the PLNT could reach several times their levels in other cases.

### Interaction Plots for the von Mises Stress

The LC modulus had a stronger influence on the levels of stress within the LC than it had on the strains (Fig. 9). Although in Figure 5 interactions between the modulus of the sclera and the moduli of the LC and PLNT were more modest than other interactions, their effects were clearly distinguishable on the interaction plots.

Variance in the Responses Described by the Influential Factors

Finally, I computed the proportion of the total variance in each of the responses accounted for by the set of the nine influential factors, and the interactions between them, over all the responses (Table 2). These variances ranged between 95% and 99.8%, depending on the response. This means that if in this
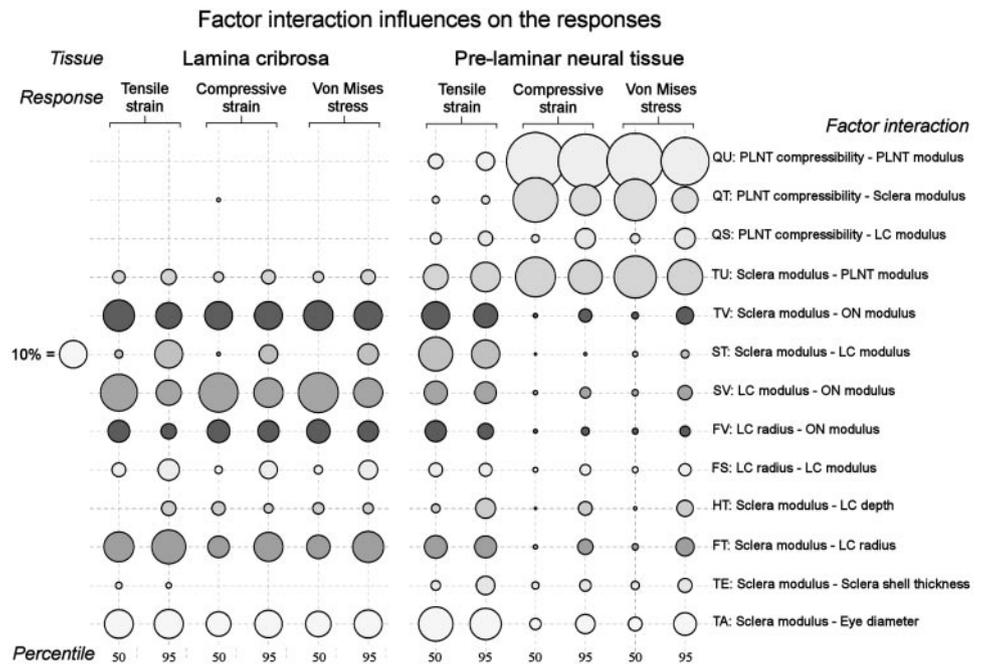
FIGURE 5. Strengths of the factor interaction influences on the responses, as a percentage of the effects of all interactions on the response. Each *row* corresponds to an interaction between two factors, and each *column* to a response. Larger discs represent more influential interactions. Of 210 two-factor interactions that could influence each response (½ · 21 · 20 = 210), those shown are statistically significant (*P* < 0.01) and contributed at least 5% to any response. Responses varied in their sensitivity to factor interactions. Examples of how the interactions affect the responses are presented in Figures 6 to 9.
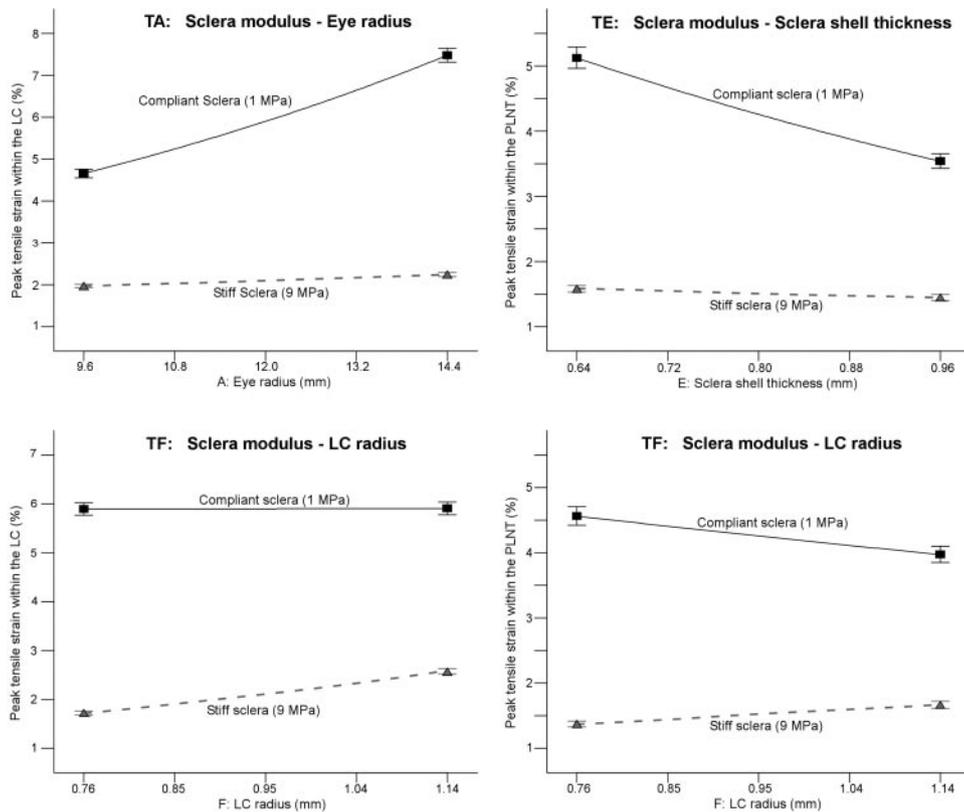
FIGURE 6. Effects on the tensile strains within the LC (*left*) and the PLNT (*right*) of interactions involving scleral modulus. The effects of some factors changed substantially depending on whether the sclera was stiff (*dashed lines*) or compliant (*continuous lines*). Some factors, such as eye size (*top left*) or sclera shell thickness (*top right*), had virtually no influence if the sclera was stiff (*horizontal lines*), but could lead to changes in strain if the sclera was compliant (*steep lines*). The LC radius, in contrast, had a different interaction with the scleral modulus. When the sclera was stiff, increased LC radius led to increases in strain on both the LC (*bottom left*) and the PLNT (*bottom right*). When the sclera was compliant, LC radius had no influence on the LC, but it did affect the PLNT in the opposite way as if the sclera was stiff. Conversely, it is possible to deduct the effects of changes in sclera modulus from the distance between the *dashed* and *continuous lines.* The influence of the sclera modulus was generally large, but its strength depended on other factors, and it affected the LC differently than it affected the PLNT.

work only the nine most influential factors had been examined, at least 95% of the variance in the responses would still have been captured).

DISCUSSION

The goal of this study was to determine the relative strength of the influences of factors, independently and in interaction, on the ONH mechanical response to changes in IOP. The two most important results were: first, that there were strong interactions, meaning that the effects of some factors were substantially different depending on other factors. Second, that despite the strong influence of the sclera on ONH biomechanics, its effects depended on, and could be outweighed by, other factors. This meant that strains within the LC or PLNT could be elevated when the sclera was stiff, or the strains could be low when the sclera was compliant. The various aspects of the ONH response were sensitive to different factors, but a set of nine factors, and the interactions between them, accounted for between 95% and 99.8% of the total variance in the responses. The influential factors included the properties of the sclera (modulus, eye radius, and shell thickness), LC (modulus and radius), PLNT (modulus and compressibility), and ON (modulus) and IOP. The rest of the factors had effects that were either much weaker or not statistically significant. Although this author and others[2,5,12,20] have speculated about factor interactions, to the best of the author's knowledge, this study is the first to focus on factor interactions on the ONH. It is hoped that this information will provide insights into the origin of the range of sensitivities to elevated IOP and that it will help focus future modeling and experimental studies of ocular biomechanics.

Scleral properties had a strong influence on all responses. The reason being that the sclera is the main load-bearing tissue of the eye.[12,18,27–30] If the deformation experienced by the sclera for a given level of IOP changes, then what it transmits to the ONH also changes. Under a given load, the deformation experienced by the sclera is a combination of its mechanical properties (modulus) and geometry (mainly its thickness and the eye radius). Since decreases in eye radius or increases in shell thickness may reduce the deformation of the sclera, these factors could be said to change the effective, or structural, scleral stiffness.

The scleral modulus interacted with several other factors, sometimes splitting the effects of the second factor into two regimens. For example, variations in eye radius or in shell thickness influenced the levels of strain and stress within the ONH when the sclera was compliant, but not when it was stiff. Similarly, depending on scleral stiffness, the influences of LC radius or PLNT compressibility could change and even switch directions from increasing to decreasing a response.

Identifying the important interactions involving properties of the sclera may be of interest in the search for associations between ocular properties and risk or sensitivity to IOP, particularly since the ocular hypertension treatment study (OHTS) found that central corneal thickness (CCT) was an independent factor in the development of glaucomatous optic neuropathy.[31–33] The origin of this result is still not understood. An often-mentioned hypothesis is that perhaps CCT is a surrogate of other properties of the sclera or LC, such that a structurally weak (either compliant or thin) cornea could correspond to a structurally weak sclera or LC, leading to a mechanically sensitive ONH.[2,33–37] However, despite efforts,[35,36,38] the relationship between cornea and sclera or LC is still unclear. Oliveira et al.[38] found no correlations between CCT and anterior sclera thickness or axial length. Jonas and Holbach[36] found that in nonglaucomatous human globes, CCT did not correlate with LC or peripapillary sclera thickness, and concluded that "susceptibility to glaucoma cannot be explained by an anatomic correspondence between corneal thickness and histomorphometry of the optic nerve head." Wells et al.[35] found that corneal hysteresis, but not CCT, or other of the corneal parameters they measured, was associated with increased deformation of the optic nerve surface during elevations of IOP. These
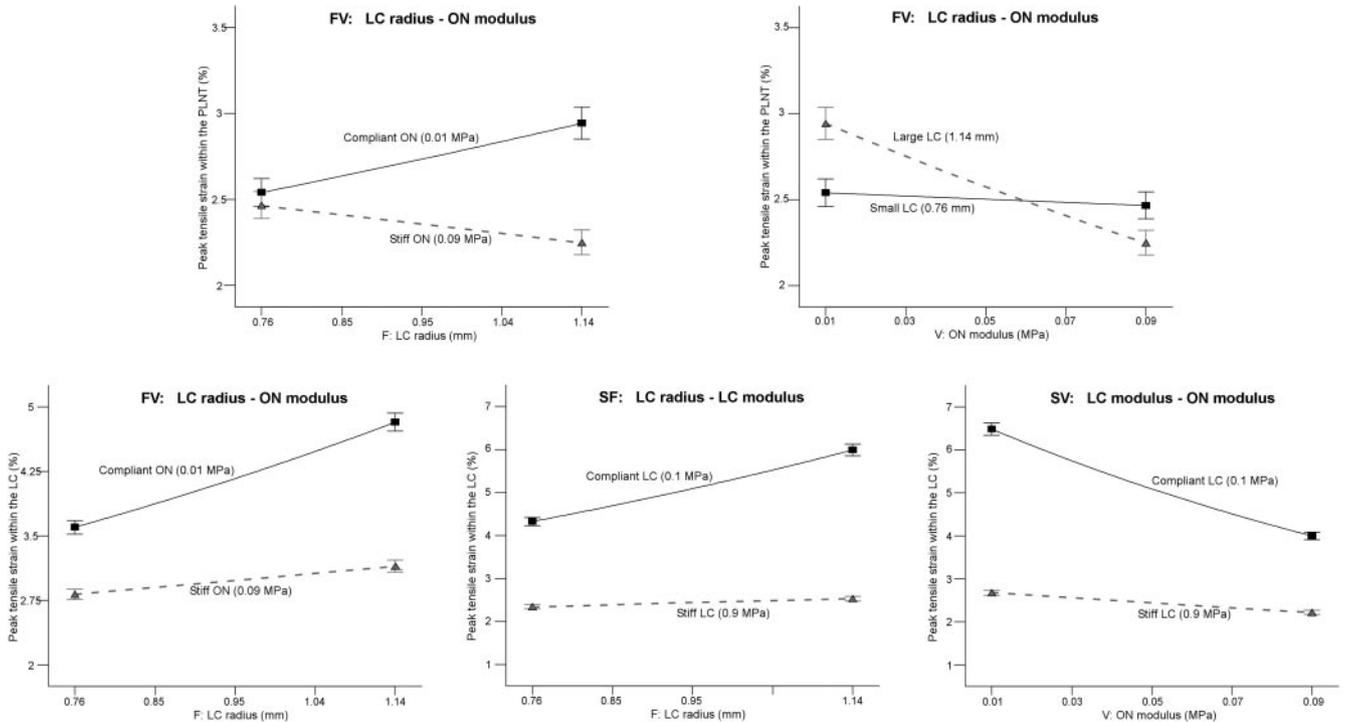
FIGURE 7. Effects on the tensile strains of interactions not involving the sclera. *Top two panels*: orthogonal perspectives that illustrate two aspects of the interaction between LC radius and ON modulus: the effects of increases in LC radius depended on the compliance of the ON, and, conversely, the effects of ON compliance depended on the LC radius. Increases in LC radius led to increases in tensile strains within the PLNT if the ON was compliant, or to decreases if the ON was stiff. Similarly, for an LC with small radius, ON compliance did not affect the strain within the PLNT, whereas for a large LC an increase in ON modulus produced a decrease in PLNT tensile strain. *Bottom row*: increases in LC radius or compliance led to increases in peak tensile strain, albeit the combined effects of changes in ON modulus and LC size were larger than the simple superposition. Similar to what is shown for the sclera in Figure 6, increases in LC radius had no effect on peak tensile strain within the LC if the LC was stiff, but did increase the strains if the LC was compliant. *Bottom right*: stiffening of the ON reduced the peak tensile strains within the LC, more so for compliant LCs than for stiff LCs where the strain was already low.

studies are valuable, but they may be more fruitful if factor interactions are considered. According to the interactions shown herein, the influence of the sclera thickness and axial length decreases dramatically as the sclera modulus increases, which could mean that sclera thickness and axial length correlate with IOP-induced changes in the ONH surface in eyes with a compliant sclera, but not in eyes with a stiff sclera.

The author is not proposing that this is the first work to note that factor effects sometimes depend on each other. For example, studies of corneal response to loading, such as during applanation tonometry, have found that corneal thickness and mechanical properties have to be considered simultaneously, because their effects are not independent.[39] It is common to show plots in which more than one factor is varied. Investigators, however, generally do not explore the interactions, missing the insight that these may provide, or leaving the readers with the impression that these are intractable complications. This study shows that, despite the complexity of ONH biomechanics, it is possible to study and quantify factor interactions in a systematic way. Computational models, even when simplified, provide an ideal platform to explore ocular biomechan-

FIGURE 8. Illustration of the effects of interactions on the peak (*left*) and median (*right*) compressive strains within the PLNT. The effects of PLNT compressibility were complex, as it was involved in several interactions. The figure illustrates its interactions with the moduli of the sclera and PLNT, both classic examples of interactions. *Left*: the effects of PLNT compressibility inverted depending on the stiffness of the sclera. Decreasing compressibility (increased Poisson ratio) led to decreases in compressive strains, if the sclera was stiff (*dashed lines*), but to increases in compressive strains if the sclera was compliant (*continuous lines*). Conversely, from the distance between the lines, the effects of sclera modulus were larger in an incompressible PLNT (high Poisson ratio), than in a compressible PLNT (low Poisson ratio). *Right*: for a stiff PLNT, the compressibility only had a marginal effect. But for a compliant PLNT an increase in compressibility produced a huge increase in strain. Clearly the effects of PLNT modulus were larger in a compressible PLNT than in an incompressible PLNT.
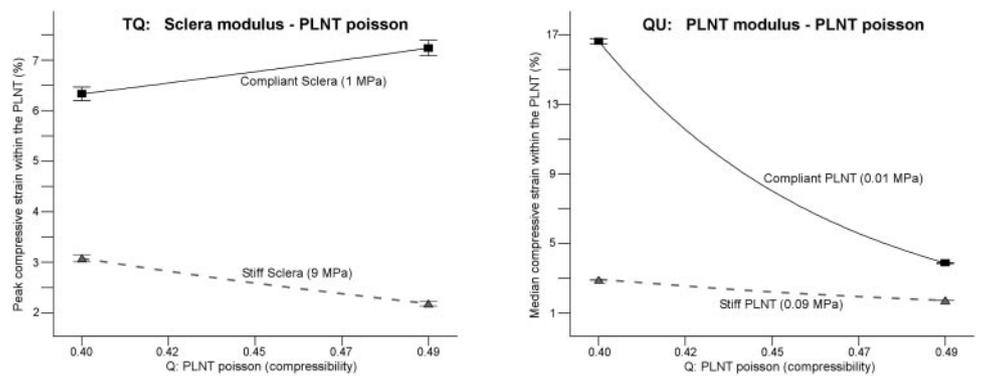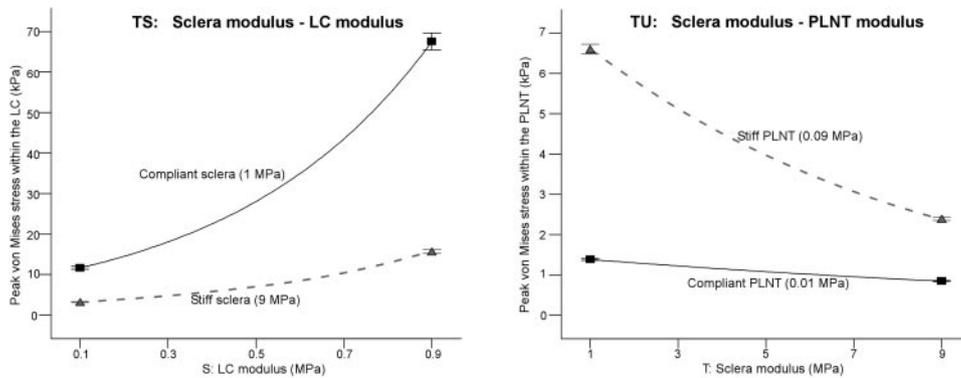
FIGURE 9. Interactions affecting the peak von Mises stresses within the LC (*left*) and PLNT (*right*). Stiffening of the LC increased the stress levels within the LC, much more so when the sclera was compliant than when it was stiff. Similarly, variations of scleral modulus had a stronger effect on LC stresses when the LC was stiff, than when the LC was compliant. This result showcases the much larger effect of the sclera on the LC than the other way around. A similar situation occurred with stresses within the PLNT: PLNT modulus was more influential if the sclera was compliant, and scleral modulus was more influential if the PLNT was stiff.

ics and identify the key factors and their interactions to inform experimental design and analysis.

Despite the strong influence of scleral stiffness, its effects can be outweighed by other factors, such that the levels of IOP-induced strain within the LC and PLNT could be high when the sclera is stiff or low when the sclera is compliant. Even more, some influential interactions did not involve scleral properties, like those including LC radius and the moduli of LC and ON. These interactions illustrate how the LC and PLNT could be supported mechanically by the underlying structures, if needed. More compliant or larger LCs relied more on the ON for support and therefore were more sensitive to ON modulus. These structures could also be more susceptible to the levels of CSF pressure.[40–43] However, analysis of this possibility requires models incorporating CSF.

In the current study, unlike in previous ones, the properties of the PLNT, both independently and in interaction, were among the most influential factors. When the PLNT was (relatively) stiff, it made no difference whether the tissue was incompressible or not. However, when the PLNT was compliant, the compressive strains, but not the tensile strains, depended strongly on the tissue compressibility. In prior OFAT studies, no substantial influence of PLNT factors was found.[12,20] These results are not contradictory; it is an example of the benefits of two improvements of this work compared with previous work: First, adding the compressive strains as a response of interest revealed influential factors that had been missed because they did not influence the tensile strains. Second, use of a fractional factorial sampling strategy allowed exploration of a much larger region of factor space and con-

sideration of a compliant and compressible PLNT. However, the rationale for allowing PLNT tissue compressibility must be noted. Compressibility in this work was intended to model the changes in PLNT volume associated with IOP increases, for example, due to altered vascular volume and perfusion or axoplasmic flow.[2,44–48] Recall that the PLNT in this work included the choroid, which at elevated IOP may be unable to retain volume. Studies of brain tissue have found it to be "nearly incompressible."[49] The differential effects of PLNT properties on tensile and compressive strains could be important because experiments on neurons and astrocytes have established that cell sensitivity to mechanical stimulation depends on the type, magnitude, and temporal profile of the stimulus.[50–56] The magnitude of the effects of the properties of the PLNT was somewhat surprising, especially because so little is known about them.

Limitations

The author has previously discussed the limitations and most salient consequences of the choices of model geometry and mechanical properties,[11,18] of the factors and their ranges,[12,20] and of the responses analyzed,[7,12,20] and so these will not be discussed at length again. Instead, below is a summary of earlier discussions, with a focus on the limitations and considerations most relevant to this work.

The tissues were assumed to be mechanically homogeneous, linear, and isotropic. Evidence suggests that these are only approximations and that the tissues are inhomogeneous,[57–60] nonlinear,[27,61–63] and anisotropic.[27,60,63–66]

TABLE 2. Cumulative Percentage of the Response Variance Described by the Nine Most Influential Factors, and Their Interactions

	Lamina Cribrosa						Prelaminar Neural Tissue					
	Tensile Strain		Compressive Strain		Von Mises Stress		Tensile Strain		Compressive Strain		Von Mises Stress	
	50th	95th	50th	95th	50th	95th	50th	95th	50th	95th	50th	95th
Factors	94.1	87.1	95.3	93.5	96.7	95.5	91.5	8.7	87.0	82.4	86.1	87.0
Interactions	3.7	9.0	2.2	3.8	1.8	2.8	6.6	16.4	12.8	15.7	13.7	11.2
Factors + interactions	97.8	96.1	97.5	97.3	98.5	98.4	98.2	95.0	99.8	98.1	99.8	98.2

The proportion of the total variance of each of the responses accounted for by the nine most influential factors, independently, through interaction with other factors in the set, or combined. Numbers are rounded to one decimal place. The nine most influential factors were: the properties of the sclera (modulus, eye diameter and shell thickness), LC (modulus and radius), PLNT (modulus and compressibility), ON (modulus), and IOP.

The interactions identified in this work are particularly interesting in the context of scleral mechanical nonlinearity. In a nonlinear sclera, increases in IOP induce strain and stress and lead to an increase in scleral modulus.[27,61–63] This brings about a shift in the influences of the various factors that interact with the scleral modulus. In this work, the use of linear mechanical properties decoupled the effects of IOP and scleral modulus. Consequently, no interactions involving IOP were found. As more complex mechanical properties are incorporated into the models, an effort already in progress, IOP is expected to interact with other factors. The lessons learned from these simplified models may help in understanding models with more complex and physiologically accurate properties.

The models in the current study represent an acute deformation of the tissues due to increases in IOP and do not account for the long-term remodeling processes that are known to take place as glaucoma develops.[53,67,68] In this work, as in previous studies,[6,12,18] the highest magnitudes of strain were predicted in the neural tissue regions, not in the LC where damage to the retinal ganglion cells (RGCs) seems to initiate in glaucoma.[69–73] This could be because with a homogeneous LC, the models presented herein could not account for the effects of the LC microarchitecture, which may amplify the levels of strain (Downs J, et al. *IOVS* 2007;48:ARVO E-Abstract 3301). It is also possible that the RGC axons are not equally sensitive to, or equally capable of recovering from, mechanical stimulation in all regions of the ONH.

The models were based on a simplified axisymmetric geometry, and therefore do not completely reflect the complex architecture of the ONH region or the corneoscleral shell (which is not of constant thickness), which could affect the mechanical interactions between the constitutive tissues. In addition, the ONH geometry differs between individuals in more complex ways that can be captured by the factors considered.[19,74–76] The biomechanical effects of the details of the geometry have been studied using OFAT techniques and individual-specific models based on human donor eyes.[6,7,11,20] It was found that the details of the geometry had a modest influence compared with that of mechanical properties.

Further Considerations on the Choice of Design, Factors, and Responses

The two-level fractional factorial experimental design used in this study is common in screening analyses.[21,22] A full factorial analysis (all the combinations) on 21 factors at two levels would have required $2^{21} = 2,097,152$ models. The 2^{21-12} fractional factorial design enabled the study to be performed with a subset of only 512 configurations (plus centers), a 1/4096th fraction, saving considerable time, but at a cost: It was not possible to resolve all possible factor effects. Those unresolved become confounded, or aliased, with other effects.[21,22] A careful design allowed the confounded effects to be only those of higher order interactions. The smaller the fraction of factor combinations studied, the more factor effects are confounded—a property called the design "resolution." In a resolution V design, like the one used in this work, no main effects or two-factor interactions are confounded with each other.[21,22] It was found during the analysis that no three-factor interaction had a strong and statistically significant influence, and therefore the discussion elsewhere was limited to independent factors and their two-factor interactions. Herein, 21 factors were studied, but the methodology can be extended to many more (even hundreds[77]). There are other factorial designs requiring fewer runs, such those of Taguchi or Plackett-Burman,[26] but it was not the purpose of this study to identify the minimum number of configurations necessary for the analysis. The design was chosen because it has an amenable mix of efficiency, robustness, and clarity.

All the configurations, except the center one, were at the corners of the factor space, which meant that it was only possible to approximate the curvature of the response dependences on the factors.[22] A general linear model (equivalent to a multivariate linear regression) was fit to each of the responses by using the parameters estimated by the ANOVA,[21,22,26] with excellent correspondence ($R^2 > 0.97$ and $P < 0.0001$ for all responses). However, a lack-of-fit test at the center configuration was significant ($P < 0.01$ for all responses). This means that the factorial analysis in this work successfully established overall factor influences, but also that it was unable to determine accurately the response curvatures—not surprising considering the curvature in responses observed in previous OFAT studies.[12,18,20] A second-phase analysis with more factor levels, which allows a better fit of the curvature, is already under way.

As mentioned earlier, the physiologically accurate ranges for the factors studied here are not completely known, and therefore assumptions had to be made that could potentially influence the results. An unnaturally large range could make a factor artificially influential, and conversely make other factor influences modest. An attempt was made to mitigate this problem by varying, when possible, similar factors over the same proportional ranges.[12,20] The choice of ranges and factorial analysis allowed some combinations of factors that produced levels of strain that appear too high to be physiologic. Without more information about the mechanical properties of the tissues of the ONH, of how they vary with other factors, and of which levels of strain or stress are unrealistic, it is impossible to determine a priori which combinations of factors are unrealistic. For this reason, and because the intention was in part to help guide future experimental work, these configurations were not excluded from the analysis.

The choice of responses also merits further discussion. These were chosen because studies in mechanobiology have suggested that some tissues are sensitive to them and therefore are potentially biologically relevant.[49,78–82] Previous works[7,83] have reported and discussed the complexity of the mechanical response of the ONH to acute increases in IOP, the need to differentiate between tensile and compressive strains, as well as the need to distinguish the strain from the stress. This work was focused on the LC and PLNT because previous studies have shown that they exhibit the largest median and peak strains, respectively.[7,11,12] Also, the LC is of interest since it is where insult to the RGC axons is believed to initiate.[69–71] Unfortunately, however, the physiologically relevant response is still unknown.[2,7] Therefore, the choice of responses, although based on an understanding of the physiology of the ONH, was ultimately arbitrary. Nevertheless, the author believes that the responses chosen are indicative of some of the fundamental aspects of the mechanical effects of IOP on the ONH, whether or not they represent the actual path or biological effect leading to the disease.

The simplified geometry and mechanical properties we have assumed provide a reasonable first approximation that allows improved understanding of ONH biomechanics. Like other computational studies, the results presented herein are, by nature, preliminary, because the choices may affect the results. As more information regarding the mechanical properties and physiologic ranges of the tissues and geometries modeled is obtained, and the effects of mechanostimulation of the ONH are better characterized, it will be necessary to update this work. Some results will change. The factor interactions identified herein may be reinterpreted, or new ones may be found. Nevertheless, the author believes that the main conclusion of this work is robust and will remain valid—namely, that factor interactions occur and can be identified and analyzed. Once this point is accepted, it becomes clear that the most appropriate approach for the study of ocular biomechanics is to consider the effects of interactions between factors.

Acknowledgments

References

1. Quigley HA. Number of people with glaucoma worldwide. *Br J Ophthalmol.* 1996;80:389–393.

2. Burgoyne CF, Downs JC, Bellezza AJ, Suh JK, Hart RT. The optic nerve head as a biomechanical structure: a new paradigm for understanding the role of IOP-related stress and strain in the pathophysiology of glaucomatous optic nerve head damage. *Prog Retin Eye Res.* 2005;24:39–73.

3. Geijssen HC. *Studies on Normal Pressure Glaucoma.* New York: Kugler Publications; 1991:240.

4. Bellezza AJ, Hart RT, Burgoyne CF. The optic nerve head as a biomechanical structure: initial finite element modeling. *Invest Ophthalmol Vis Sci.* 2000;41:2991–3000.

5. Sander EA, Downs JC, Hart RT, Burgoyne CF, Nauman EA. A cellular solid model of the lamina cribrosa: mechanical dependence on morphology. *J Biomech Eng.* 2006;128(6):879–889.

6. Sigal IA, Flanagan JG, Tertinegg I, Ethier CR. Reconstruction of human optic nerve heads for finite element modeling. *Technol Health Care.* 2005;13:313–329.

7. Sigal IA, Flanagan JG, Tertinegg I, Ethier CR. Predicted extension, compression and shearing of optic nerve head tissues. *Exp Eye Res.* 2007;85:312–322.

8. Dongqi H, Zeqin R. A biomathematical model for pressure-dependent lamina cribrosa behavior. *J Biomech.* 1999;32:579–584.

9. Edwards ME, Good TA. Use of a mathematical model to estimate stress and strain during elevated pressure induced lamina cribrosa deformation. *Curr Eye Res.* 2001;23:215–225.

10. Bellezza AJ. Biomechanical properties of the normal and early glaucomatous optic nerve head: an experimental and computational study using the monkey model. New Orleans, LA: Department of Biomedical Engineering, Tulane University; 2002. Thesis.

11. Sigal IA, Flanagan JG, Tertinegg I, Ethier CR. Modeling individual-specific human optic nerve head biomechanics.r Part I: IOP-induced deformations and influence of geometry. *Biomech Model Mechanobiol.* Published online February 29, 2008.

12. Sigal IA, Flanagan JG, Ethier CR. Factors influencing optic nerve head biomechanics. *Invest Ophthalmol Vis Sci.* 2005;46:4189–4199.

13. Czitrom V. One-factor-at-a-time versus designed experiments. *Am Statist.* 1999;53:126–131.

14. Dar FH, Aspden RM. A finite element model of an idealized diarthrodial joint to investigate the effects of variation in the mechanical properties of the tissues. *Proc Inst Mech Eng* [*H*]. 2003;217: 341–348.

15. Dar FH, Meakin JR, Aspden RM. Statistical methods in finite element analysis. *J Biomech.* 2002;35:1155–1161.

16. Yang K, Teo EC, Fuss FK. Application of Taguchi method in optimization of cervical ring cage. *J Biomech.* 2007;40:3251–3256.

17. Beillas P, Lee SW, Tashman S, Yang KH. Sensitivity of the tibio-femoral response to finite element modeling parameters. *Comput Methods Biomech Biomed Eng.* 2007;10:209–221.

18. Sigal IA, Flanagan JG, Tertinegg I, Ethier CR. Finite element modeling of optic nerve head biomechanics. *Invest Ophthalmol Vis Sci.* 2004;45:4378–4387.

19. Sigal IA. Human optic nerve head biomechanics: an analysis of generic and individual-specific models using the finite element method. Toronto, ON, Canada: Department of Mechanical and Industrial Engineering, University of Toronto; 2006. Thesis.

20. Sigal IA, Flanagan JG, Tertinegg I, Ethier CR. Modeling individual-specific human optic nerve head biomechanics. Part II: influence of material properties. *Biomech Model Mechanobiol.* Published online February 27, 2008.

21. Montgomery DC. *Design and Analysis of Experiments*. New York: Wiley; 2004:660.

22. Anderson MJ, Whitcomb PJ. *DOE Simplified: Practical Tools for Effective Experimentation*. Florence, KY: Productivity Press; 2000:256.

23. Yao J, Salo AD, Lee J, Lerner AL. Sensitivity of tibio-menisco-femoral joint contact behavior to variations in knee kinematics. *J Biomech.* 2008;41:390–398.

24. Anderson MJ, Whitcomb PJ. *RSM Simplified: Optimizing Processes Using Response Surface Methods for Design of Experiments*. Florence, KY: Productivity Press; 2005:292.

25. Nelder JA. The selection of terms in response-surface models: how strong is the weak-heredity principle? *Am Statist.* 1998;52:315.

26. Box GEP, Hunter JS, Hunter WG. *Statistics for Experimenters: Design, Innovation, and Discovery*. 2nd ed. New York: Wiley-Interscience; 2005:664.

27. Girard M, Downs J, Bottlang M, Burgoyne CF, Suh JK. An anisotropic hyperelastic constitutive model for ocular soft-tissues, Part II. Application to monkey posterior sclera. *J Biomechan Eng.* 2008;19.

28. Downs JC, Blidner RA, Bellezza AJ, Thompson HW, Hart RT, Burgoyne CF. Peripapillary scleral thickness in perfusion-fixed normal monkey eyes. *Invest Ophthalmol Vis Sci.* 2002;43:2229–2235.

29. Downs JC, Ensor ME, Bellezza AJ, Thompson HW, Hart RT, Burgoyne CF. Posterior scleral thickness in perfusion-fixed normal and early-glaucoma monkey eyes. *Invest Ophthalmol Vis Sci.* 2001;42: 3202–3208.

30. Woo SL, Kobayashi AS, Lawrence C, Schlegel WA. Mathematical model of the corneo-scleral shell as applied to intraocular pressure-volume relations and applanation tonometry. *Ann Biomed Eng.* 1972;1:87–98.

31. Gordon MO, Beiser JA, Brandt JD, et al. The Ocular Hypertension Treatment Study: baseline factors that predict the onset of primary open-angle glaucoma. *Arch Ophthalmol.* 120:714–720, 2002; discussion 829–730.

32. Herndon LW, Weizer JS, Stinnett SS. Central corneal thickness as a risk factor for advanced glaucoma damage. *Arch Ophthalmol.* 2004;122:17–21.

33. AGIS Investigators. The Advanced Glaucoma Intervention Study (AGIS): 7. The relationship between control of intraocular pressure and visual field deterioration. *Am J Ophthalmology* 2000;130: 429.

34. Meredith SP, Swift L, Eke T, Broadway DC. The acute morphologic changes that occur at the optic nerve head induced by medical reduction of intraocular pressure. *J Glaucoma.* 2007;16:556–561.

35. Wells AP, Garway-Heath DF, Poostchi A, Wong T, Chan KC, Sachdev N. Corneal hysteresis but not corneal thickness correlates with optic nerve surface compliance in glaucoma patients. *Invest Ophthalmol Vis Sci.* 2008;49:3262–3268.

36. Jonas JB, Holbach L. Central corneal thickness and thickness of the lamina cribrosa in human eyes. *Invest Ophthalmol Vis Sci.* 2005; 46:1275–1279.

37. Lesk MR, Spaeth GL, Azuara-Blanco A, et al. Reversal of optic disc cupping after glaucoma surgery analyzed with a scanning laser tomograph. *Ophthalmology.* 1999;106:1013–1018.

38. Oliveira C, Tello C, Liebmann J, Ritch R. Central corneal thickness is not related to anterior scleral thickness or axial length. *J Glaucoma.* 2006;15:190–194.

39. Liu J, Roberts CJ. Influence of corneal biomechanical properties on intraocular pressure measurement: quantitative analysis. *J Cataract Refract Surg.* 2005;31:146–155.

40. Morgan WH, Yu DY, Cooper RL, Alder VA, Cringle SJ, Constable IJ. The influence of cerebrospinal fluid pressure on the lamina cribrosa tissue pressure gradient. *Invest Ophthalmol Vis Sci.* 1995; 36:1163–1172.

41. Morgan WH, Yu DY, Cooper RL, Alder VA, Cringle SJ, Constable IJ. Retinal artery and vein pressures in the dog and their relationship to aortic, intraocular, and cerebrospinal fluid pressures. *Microvasc Res.* 1997;53:211–221.

42. Jonas JB, Berenshtein E, Holbach L. Anatomic relationship between lamina cribrosa, intraocular space, and cerebrospinal fluid space. *Invest Ophthalmol Vis Sci.* 2003;44:5189–5195.

43. Berdahl JP, Allingham RR, Johnson DH. Cerebrospinal fluid pressure is decreased in primary open-angle glaucoma. *Ophthalmology.* 2008;115:763–768.

44. Anderson DR, Hendrickson A. Effect of intraocular pressure on rapid axoplasmic transport in monkey optic nerve. *Invest Ophthalmol.* 1974;13:771–783.

45. Minckler DS, Bunt AH, Johanson GW. Orthograde and retrograde axoplasmic transport during acute ocular hypertension in the monkey. *Invest Ophthalmol Vis Sci.* 1977;16:426–441.

46. Hahnenberger RW. Effects of pressure on fast axoplasmic flow: an in vitro study in the vagus nerve of rabbits. *Acta Physiol Scand.* 1978;104:299–308.

47. Bilston LE. The effect of perfusion on soft tissue mechanical properties: a computational model. *Comput Methods Biomech Biomed Eng.* 2002;5:283–290.

48. Findl O, Strenn K, Wolzt M, et al. Effects of changes in intraocular pressure on human ocular haemodynamics. *Curr Eye Res.* 1997; 16:1024–1029.

49. Edwards ME, Wang SS, Good TA. Role of viscoelastic properties of differentiated SH-SY5Y human neuroblastoma cells in cyclic shear stress injury. *Biotechnol Prog.* 2001;17:760–767.

50. Kirwan RP, Crean JK, Fenerty CH, Clark AF, O'Brien CJ. Effect of cyclical mechanical stretch and exogenous transforming growth factor-beta1 on matrix metalloproteinase-2 activity in lamina cribrosa cells from the human optic nerve head. *J Glaucoma.* 2004; 13:327–334.

51. Kirwan RP, Fenerty CH, Crean J, Wordinger RJ, Clark AF, O'Brien CJ. Influence of cyclical mechanical strain on extracellular matrix gene expression in human lamina cribrosa cells in vitro. *Mol Vis.* 2005;11:798–810.

52. Ellis EF, McKinney JS, Willoughby KA, Liang S, Povlishock JT. A new model for rapid stretch-induced injury of cells in culture: characterization of the model using astrocytes. *J Neurotrauma.* 1995;12:325–339.

53. Hernandez MR. The optic nerve head in glaucoma: role of astrocytes in tissue remodeling. *Prog Retin Eye Res.* 2000;19:297–321.

54. Morgan JE. Optic nerve head structure in glaucoma: astrocytes as mediators of axonal damage. *Eye.* 2000;14:437–444.

55. Neufeld AH, Sawada A, Becker B. Inhibition of nitric-oxide synthase 2 by aminoguanidine provides neuroprotection of retinal ganglion cells in a rat model of chronic glaucoma. *Proc Natl Acad Sci U S A.* 1999;96:9944–9948.

56. Ostrow LW, Langan TJ, Sachs F. Stretch-induced endothelin-1 production by astrocytes. *J Cardiovasc Pharmacol.* 2000;36:S274–S277.

57. Curtin BJ. Physiopathologic aspects of scleral stress-strain. *Trans Am Ophthalmol Soc.* 1969;67:417–461.

58. Quigley HA, Addicks EM. Regional differences in the structure of the lamina cribrosa and their relation to glaucomatous optic nerve damage. *Arch Ophthalmol.* 1981;99:137–143.

59. Quigley HA, Dorman-Pease ME, Brown AE. Quantitative study of collagen and elastin of the optic nerve head and sclera in human and experimental monkey glaucoma. *Curr Eye Res.* 1991;10:877–888.

60. Roberts MD, Grau V, Grimm J, et al. Remodeling of the connective tissue microarchitecture of the lamina cribrosa occurs early in experimental glaucoma in the monkey eye. *Invest Ophthalmol Vis Sci.* 2009 Feb;50(2):681–690.

61. Spoerl E, Boehm AG, Pillunat LE. The influence of various substances on the biomechanical behavior of lamina cribrosa and peripapillary sclera. *Invest Ophthalmol Vis Sci.* 2005;46:1286–1290.

62. Woo SL, Kobayashi AS, Schlegel WA, Lawrence C. Nonlinear material properties of intact cornea and sclera. *Exp Eye Res.* 1972; 14:29–39.

63. Girard MJ, Downs JC, Burgoyne CF, Suh JK. Experimental surface strain mapping of porcine peripapillary sclera due to elevations of intraocular pressure. *J Biomech Eng.* 2008;130:041017.

64. Rada JA, Shelton S, Norton TT. The sclera and myopia. *Exp Eye Res.* 2006;82:185–200.

65. Komai Y, Ushiki T. The three-dimensional organization of collagen fibrils in the human cornea and sclera. *Invest Ophthalmol Vis Sci.* 1991;32:2244–2258.

66. Watson PG, Young RD. Scleral structure, organisation and disease: a review. *Exp Eye Res.* 2004;78:609–623.

67. Hernandez MR, Andrzejewska WM, Neufeld AH. Changes in the extracellular matrix of the human optic nerve head in primary open-angle glaucoma. *Am J Ophthalmol.* 1990;109:180–188.

68. Morrison JC, Dorman-Pease ME, Dunkelberger GR, Quigley HA. Optic nerve head extracellular matrix in primary optic atrophy and experimental glaucoma. *Arch Ophthalmol.* 1990;108:1020–1024.

69. Gaasterland D, Tanishima T, Kuwabara T. Axoplasmic flow during chronic experimental glaucoma. 1. Light and electron microscopic studies of the monkey optic nervehead during development of glaucomatous cupping. *Invest Ophthalmol Vis Sci.* 1978;17:838–846.

70. Quigley HA, Addicks EM. Chronic experimental glaucoma in primates. II. Effect of extended intraocular pressure elevation on optic nerve head and axonal transport. *Invest Ophthalmol Vis Sci.* 1980;19:137–152.

71. Quigley HA, Addicks EM, Green WR, Maumenee AE. Optic nerve damage in human glaucoma. II. The site of injury and susceptibility to damage. *Arch Ophthalmol.* 1981;99:635–649.

72. Shields B. *Textbook of Glaucoma.* 4th ed. Baltimore: Williams & Wilkins; 1997.

73. Quigley HA. Glaucoma: macrocosm to microcosm the Friedenwald lecture. *Invest Ophthalmol Vis Sci.* 2005;46:2662–2670.

74. Downs JC, Yang H, Girkin C, et al. Three dimensional histomorphometry of the normal and early glaucomatous monkey optic nerve head: neural canal and subarachnoid space architecture. *Invest Ophthalmol Vis Sci.* 2007;48:3195–3208.

75. Yang H, Downs JC, Bellezza AJ, Thompson H, Burgoyne CF. 3-D Histomorphometry of the normal and early glaucomatous monkey optic nerve head: prelaminar neural tissues and cupping. *Invest Ophthalmol Vis Sci.* 2007;48:5068–5084.

76. Yang H, Downs JC, Girkin C, et al. 3-D histomorphometry of the normal and early glaucomatous monkey optic nerve head: lamina cribrosa and peripapillary scleral position and thickness. *Invest Ophthalmol Vis Sci.* 2007;48:4597–4607.

77. Kleijnen JPC. *Design and Analysis of Simulation Experiments.* New York: Springer; 2007.

78. Bandak FA. On the mechanics of impact neurotrauma: a review and critical synthesis. *J Neurotrauma.* 1995;12:635–649.

79. LaPlaca MC, Cullen DK, McLoughlin JJ, Cargill RS 2nd. High rate shear strain of three-dimensional neural cell cultures: a new in vitro traumatic brain injury model. *J Biomech.* 2005;38:1093–1105.

80. Pedersen JA, Swartz MA. Mechanobiology in the third dimension. *Ann Biomed Eng.* 2005;33:1469–1490.

81. Tan JC, Kalapesi FB, Coroneo MT. Mechanosensitivity and the eye: cells coping with the pressure. *Br J Ophthalmol.* 2006;90:383–388.

82. Wang JH, Thampatty BP. An introductory review of cell mechanobiology. *Biomech Model Mechanobiol.* 2006;5:1–16.

83. Humphrey JD. Stress, strain, and mechanotransduction in cells. *J Biomech Eng.* 2001;123:638–641.